

SHOCK INTERACTION OF METAL PARTICLES IN CONDENSED EXPLOSIVE DETONATION

Robert C. Ripley*, Fan Zhang[†] and Fue-Sang Lien**

*Martec Ltd., 1888 Brunswick St., Suite 400, Halifax, NS, B3J 3J8, Canada

[†]Defence R&D Canada - Suffield, PO Box 4000, Stn. Main, Medicine Hat, AB, T1A 8K6, Canada

**University of Waterloo, 200 University Ave. W., Waterloo, ON, N2L 3G1, Canada

Abstract. Three-dimensional mesoscale modeling is conducted to study the two-phase momentum and heat transfer during shock and thin-detonation-front interaction with metal particles in liquid nitromethane under various particle packing configurations and inter-particle spacings. The results showed that the particle velocity after the shock is a strong function of material density ratio of liquid to metal and volume fraction of particles. In the detonation case, it also depends on the expansion rate of the detonation products. The pressure at the leading edge of particles in a closely-packed particle bed achieves more than twice that of the theoretical 1D transmission pressure and the corresponding fluid temperature reaches 3828 K, providing hot spots that are responsible for detonation propagation in these heterogeneous explosives.

Keywords: Heterogeneous matter, Mesoscale model, Multiphase detonation, Metallized explosive.

PACS: 43.35.Ei, 78.60.Mq

INTRODUCTION

Modern experimental techniques still lack the resolution necessary to gain insight into the mechanical, thermal and chemical behaviour of energetic materials under shock and detonation conditions. Mesoscale modeling of heterogeneous explosives is increasingly being used as a means to understand multiphase detonation phenomena [1, 2].

For detonation propagation in a condensed explosive with metal particles, a physical model describing the momentum and heat transfer between the explosive and particles has yet to be completely established. Zhang *et al.* [2] investigated momentum transfer resulting from shock interaction with a single particle and matrices of cylindrical particles using 2D simulations. Their results indicated significant momentum transfer from the explosive to the particles as the leading shock front crosses the particles, and that the primary factor affecting transmitted shock velocity for a single particle immersed in

an explosive is the initial material density ratio. The present work extends this finding with the goal to use 3D mesoscale calculations in packed particles matrices, which allows for investigation of the effect of volume fraction on fluid-particle momentum transmission factors. Furthermore, transmission factors for particle temperature and hot spots in the fluid phase are also investigated. Inert shocks representative of detonation pressures are considered in two-phase systems as a prerequisite to investigating heterogeneous detonation at the mesoscale.

MESOSCALE MODEL

Over the characteristic shock interaction time, defined as $\tau = D/d$, where D is the incident shock velocity and d is the particle diameter, inviscid hydrodynamic calculations can be applied at the mesoscale to investigate momentum and heat transfer. An Eulerian multiple-material model is em-

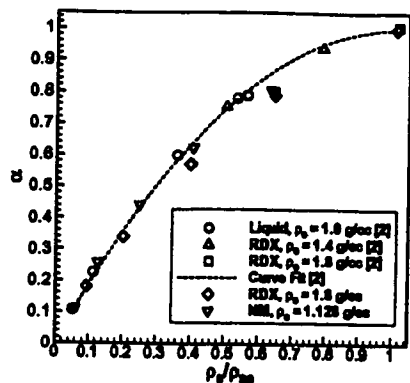


FIGURE 1. Validation of Eulerian mesoscale model.

ployed in a finite-volume framework using Cartesian grids. In this approach, the condensed explosive and particle matter are treated as a continuum, where the proportion of each is accounted for with advection of mass fraction scalars. Depending on which material is present in a computational cell, appropriate EOS parameters are applied. In cells containing multiple materials, a pressure equilibrium approach is used. Both the explosive and particle materials are modeled using a Mie-Grüneisen relationship with parameters from [3]. Temperatures are determined using the fitting technique of Walsh and Christian [4]. Material strength has been neglected by assuming that only volumetric strain occurs in the particles.

To test the mesoscale model, and validate the zero-strength assumption, shock interaction with a single spherical particle was conducted using a 2D axisymmetric grid and compared to [2]. A particle diameter of $d = 10 \mu\text{m}$ was simulated, the results of which can be scaled geometrically using inviscid assumptions. Several metals are considered for validation purposes, including Mg, Al, Ti, Cu and W, for varying initial solid densities, ρ_{S0} , where subscripts "S" and "0" denote solid particle and initial states, respectively. Liquid nitromethane (NM), and solid explosive (RDX) were used as the condensed matter to cover a range of ambient densities, ρ_0 . After [2], the shock strength employed was $P_1 = 10.1 \text{ GPa}$ with a post-shock fluid velocity $U_1 = 1.884 \text{ mm}/\mu\text{s}$. The transmission factor for velocity is $\alpha = U_S/U_1$ and for temperature is $\beta = T_S/T_1$, measured at $t = \tau$. The present results are included in Fig. 1.

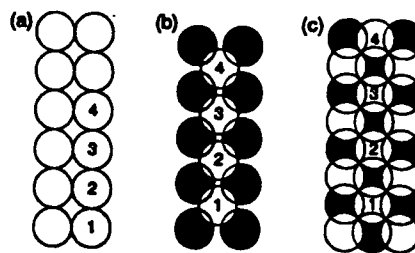


FIGURE 2. Geometric arrangements of packed particles: (a) Simple cubic (SC); (b) Body-centred (BC); and, (c) Close packed (CP).

PACKED PARTICLE MATRIX

Three volume fractions (or packing factors), ϕ , are considered for tightly-packed Al particles in NM, where there is no separation between particles. Static particle configurations are illustrated in Fig. 2.

Although the first layer of particles in the model receives a planar shock, subsequent layers are subject to non-uniform loading induced by neighboring particles and complex reflected waves. Several layers of particles are therefore required to attain quasi-steady shock propagation through the heterogeneous medium. Here, we have modeled 10 layers of packed particles and taken advantage of the periodicity of the solution by using symmetry planes. The resulting domain features quarter sphere segments placed along the intersection of symmetry planes.

Fig. 3 illustrates pressure histories observed in the close packed particle matrix ($\phi = 0.74$). At the leading edge of each layer of particles, the peak pressure is periodic between layers related to the particle packing configuration. Due to multiple shock reflections and focusing, the peak pressures are much higher than the theoretical transmission pressure of 20.9 GPa for a 1D slab. The peak pressure decays rapidly as the shock crosses the particle and then oscillates about a quasi-steady pressure. This result is representative of the three configurations tested.

Corresponding to pressure history, the mass-centred particle velocity, shown in Fig. 4, also increases rapidly as the shock crosses the particle and then oscillates about a mean value above the theoretical 1D transmission value of 1.110 mm/ μs . Results for shock velocity through the matrix and transmitted quasi-steady pressure, P_∞ are compared in Table 1, where D is measured using the arrival

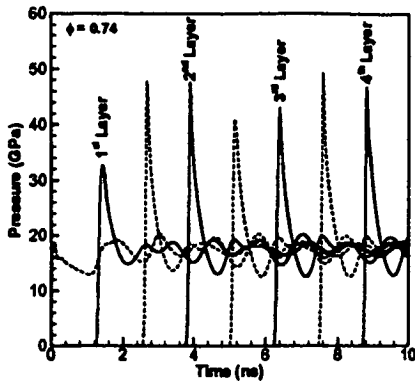


FIGURE 3. Leading edge pressure histories for NM-Al.

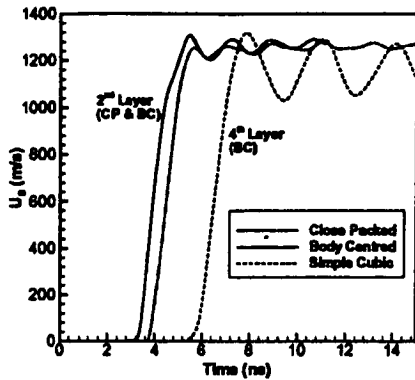


FIGURE 4. Mass-centred particle velocity for densely-packed configurations.

time and distance between each particle layer. The shock velocity for densely-packed configurations increases with volume fraction due to the particle contact, which permits shock transmission at greater velocities owing to the increased sound speed in the particle matter. Table 1 shows that the results for different volume fractions follow a trend between no particles and the theoretical transmission for 1D.

TABLE 1. Effect of volume fraction on inert shock.

Configuration	ϕ	D (mm/ μ s)	P_{∞} (GPa)
No Particles	0.00	4.769	10.1
Simple Cubic	0.52	5.486	15.1
Body-centred	0.68	5.765	17.2
Close Packed	0.74	5.969	17.9
Solid Slab (1D)	1.00	7.000	20.9

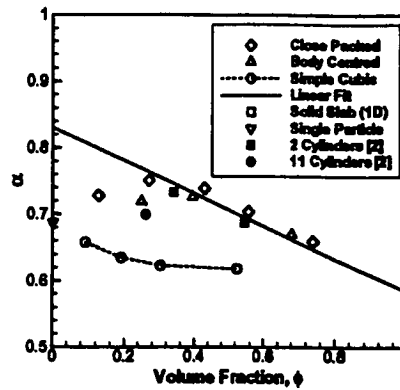


FIGURE 5. Velocity transmission factors, α , for various aluminum particle configurations in nitromethane.

Fig. 5 illustrates the present results for NM-Al for densely packed particles and with various particle spacings, ranging from 1 to 8 μ m, for each geometric particle arrangement. The results are measured after 2τ and are compared to cylindrical particle arrangements [2]. The results show that the BC and CP particle arrangements are in agreement with each other and follow a linear trend for $\phi > 0.25$ where the transmission is dominated by particle interactions, while for $\phi < 0.25$ drag effects become significant. Conversely, the SC arrangement follows a different trend with considerably lower velocity transmission factors. The SC arrangement is a limiting configuration for particles in contact that is not likely to be encountered in practice. In all cases, for ϕ approaching zero, the results tend to that of a single particle.

The temperature field shown in Fig. 6 indicates localized hot spots in the interstitial sites between particles in the matrix. The peak fluid temperature found at the particle leading edge is 3828 K in the CP configuration, while it reaches only 2383 K for the SC packing. For reactive host matter, this behaviour will significantly affect the detonation process.

DETONATION CONDITION

Condensed-phase detonation is simulated by using an additional EOS, the Jones-Wilkins-Lee (JWL) EOS [5] for the explosive detonation products and an Arrhenius reaction model using parameters from [3] to convert the condensed phase into gaseous products with an associated heat release. The JWL parameters

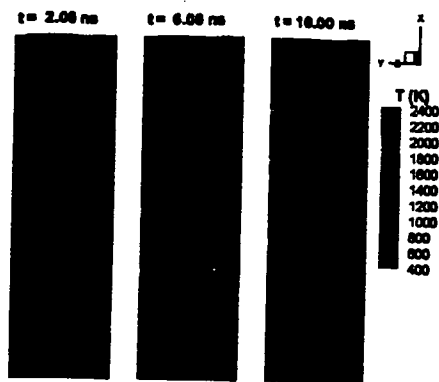


FIGURE 6. Temperature contours and particle deformation for NM-Al in close-packed matrix ($2 \mu\text{m}$ spacing).

TABLE 2. Incident shock parameters in NM and resulting transmission factors.

	Inert Shock	Reactive Shock
D (mm/ μs)	4.769	6.612
P_1 (GPa)	10.13	13.16
ρ_1 (g/cc)	1.875	1.538
U_1 (mm/ μs)	1.884	1.742
T_1 (K)	1336	3628
α	0.597	0.390
β	0.400	0.165

and burn model heat release are calculated using [6].

Transmission factors are presented for a reactive NM shock with inert Al particles. Parameters for the inert shock and detonation in NM are given in Table 2. For the detonation, the reaction zone thickness is less than $1 \mu\text{m}$ such that State 1 is taken as the CJ detonation condition.

Particle temperature is important as it often controls macro-scale particle combustion models that employ ignition temperature criteria or temperature-dependent rate laws. The temperature transmission factors are given in Table 2, which indicate a significant temperature increase in the particle as the shock crosses the particle. It has been shown for a single particle that the velocity and temperature transmission for detonation conditions are substantially different compared to particle interaction with an inert shock, due to the hot expanding detonation products in the post-shock flow (see Fig. 7).

It is noticed that the inviscid mesoscale model used here is valid for the strong inert shock interac-

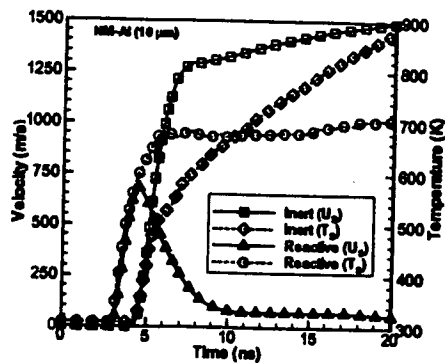


FIGURE 7. Mass-centre histories for single aluminum particle in inert and reactive NM shock.

tion with particles within the shock interaction time. For $t > \tau$, the particle is in a drag phase behind the shock and cannot be modeled rigorously without viscous fluid models. Kinetic phenomena, such as strain-rate effects or chemical reactions in the detonation case, would introduce additional length scales. If the detonation zone thickness is much smaller than the particle diameter, the current inviscid mesoscale model would still be valid within the shock interaction time. The momentum and heat transfer as the detonation front crosses the particles will be more systematically investigated for various materials of a single particle and packed particle configurations using the 3D mesoscale calculations. The influence of the conductive heating on particle temperature will also be examined considering the large temperature difference between the detonation products and the metal particle.

REFERENCES

1. Baer, M. R., *Thermochimica Acta*, 384, 351–367 (2002).
2. Zhang, F., Thibault, P. A., and Link, R., *Proceedings of the Royal Society of London, A*, 705–726 (2003).
3. Mader, C. L., *Numerical Modeling of Explosives and Propellants*, CRC Press, 1998, second edn.
4. Walsh, J. M., and Christian, R. H., *Physical Review*, 97, 1544–1556 (1955).
5. Lee, E. L., Hornig, H. C., and Kury, J. W., *Adiabatic expansion of high explosive detonation products*, University of California, LLNL UCRL-50422 (1968).
6. Fried, L. E., Howard, W. M., and Souers, P. C., *Cheetah 2.0 user's manual*, University of California, LLNL UCRL-MA-117541 Rev. 5 (1998).

525848

CA027963